

ORIGINAL ARTICLE

Antibacterial behavior of oxynitride glasses as a glassy grain boundary phase for silicon nitride-based ceramics

Seniz R. Kushan Akin¹ | Emrah Dolekcekic² | Thomas J. Webster¹

¹Department of Chemical Engineering, Northeastern University, Boston, MA, USA

²Department of Materials Science and Engineering, Eskisehir Technical University, Eskisehir, Turkey

Correspondence

Seniz R. Kushan Akin, Department of Materials Science and Engineering, Cankaya University, Ankara, Turkey. Emails: senizakin@cankaya.edu.tr; kushanakin@gmail.com

Funding information

Türkiye Bilimsel ve Teknolojik Araştırma Kurumu, Grant/Award Number: 2219

Abstract

Silicon nitride-based ceramics have provided significant advantages due to their high chemical resistance, high elastic modulus, and combination of hardness and fracture toughness (depending on self-reinforcement). Over the past two decades, a significant amount of interest has been generated for the bio-applications of these materials. However, the effect of the grain boundary phase on such applications is still not very well understood. In this study, the effect of different cations on biological (such as antibacterial and cytocompatibility) and material properties (like wetting angles and isoelectric points [IEP]) of oxynitride glasses, mimicking the grain boundary phase in Si₃N₄ and SiAlON ceramics, were investigated. Results revealed that the antibacterial behavior and mammalian cell viability were inversely correlated in glasses with rare-earth cation additions. Ca was the best cation when the two properties (bacterial response and cell proliferation) were considered together, and, thus should be further studied for a wide range of applications.

KEYWORDS

antibacterial, bioceramics, grain boundary phase, oxynitride glass, silicon nitride

1 | INTRODUCTION

In recent years, due to some of the limitations of alumina and zirconia ceramics, silicon nitride (Si₃N₄) has been investigated for structural clinical applications mainly in situations where a bone replacement is required.¹ It is clearly known that an ideal bioceramic material used for structural applications has low weight; a superior combination of fracture toughness, hardness, and strength; excellent wear resistance/tribological properties in the body environment; partially radiolucent, making it better for visualization²; and more importantly, great biological properties such as biocompatibility, osteointegration, and antibacterial properties.²⁻⁹ As a nonoxide ceramic, Si₃N₄ offers greater opportunities in all of these properties when compared with metals (e.g., Ti), oxide ceramics (e.g., Al₂O₃), and polymers (e.g., PEEK) for orthopedic and/or dental applications.¹⁰⁻¹²

Although the first study concerning Si₃N₄ biocompatibility was conducted in 1980¹³ was not encouraging, in 1989, Howlett et al¹⁴ showed that porous Si₃N₄ obtained by reaction bonding favored bone growth in vivo. Finally, in late 2018, 30 years of clinically successful outcomes of lumbar fusion surgeries performed using Si₃N₄ implants were reported.¹⁵ This was the first clinical study of Si₃N₄ as an implant material, the first commercial anterior lumbar interbody fusion with a synthetic material, the first design of a spinal interbody implant with endplate porosity to promote fusion, and the longest clinical follow-up of any implant material used in spine surgery.

Rahaman and Xiao summarized the possibility of using Si₃N₄ in healthcare until 2017.¹⁶ Afterwards, several studies were carried out to improve these materials in the biomedical field. For example, it was shown that besides the structural

importance of Si_3N_4 , clues of osteoblast cell growth on silicon nitride-based materials were identified as important to improve local healing². Further, as world-wide concerns over antibiotic resistant bacteria grow, physicochemical reactions between a gram-positive bacteria (*Staphylococcus epidermidis*) and Si_3N_4 were also investigated, and it was observed that the surface chemistry of Si_3N_4 may prevent periprosthetic infections by hindering biofilm formation and bacterial proliferation.¹⁷ The same study also revealed, one more time, that although a micron rough surface promotes the adhesion and colonization of bacteria, nano-roughness can reverse this phenomenon.

In another study, zirconia toughened alumina (ZTA) and Si_3N_4 were compared as femoral heads against ultrahigh molecular weight polyethylene (UHMWPE), and the results showed that Si_3N_4 acted as a better candidate for such use as a stable silanol layer forms in a friction and heat activated environment, whereas ZTA can become highly defective.¹⁸ Si_3N_4 was also added to 45S5 Bioglass to improve osseointegrative and osseoconductive behavior, and it promoted the formation of higher amounts of bone tissue when compared to undoped bioglass.¹⁹ For a similar purpose, functionalizing surfaces to increase bioactivity was provided by cavity formation via laser-patterning and filling the cavities with mixtures of bioglass and Si_3N_4 powder whereas adding a minor fraction of Si_3N_4 to bioglass led to larger cell colonization and to a more balanced composition of mineralized tissue.³ Mechanical and antibacterial properties of Si_3N_4 were also studied by another group as a composite with tetra needle like ZnO (T-ZnOw) whiskers.²⁰ Although the mechanical properties were slightly lower than those of samples without T-ZnOw addition, superior antibacterial properties against both *Staphylococcus aureus* (*S. aureus*) and *Escherichia coli* (*E. coli*) were observed. This behavior was attributed to the generation and release of reactive oxygen species and Zn^{2+} ions that could inhibit the growth of bacteria. Lastly, because Si_3N_4 is generally accepted as a bio inert material itself, the effect of SiO_2 , CO, and Al_2O_3 additives and the grain boundary phase they form was recently investigated.⁴ It was concluded that a change in grain boundary phase amount had a strong effect on the mechanical properties and Al_2O_3 addition was found to be advantageous via in vitro biological behavior and also mechanical properties.

It is obvious from the abovementioned studies that in recent years, improving Si_3N_4 for bio applications is of great interest. However, studies have been missing on correlating the type, amount, and structure of the sintering additives to silicon nitride-based materials on one of the most important properties of Si_3N_4 ceramics (e.g., acting as a better fixation device and the above mentioned promising biological and mechanical behavior). Because self-diffusion processes are relatively slow in Si_3N_4 -based ceramics, they require oxide sintering additives, which are generally oxides of Al, Mg, Ca,

or rare-earth metals, to provide conditions for liquid phase sintering. During sintering, the additive reacts with silica on the surface of the Si_3N_4 and some of the nitride to form an oxynitride liquid, which, when cooled, remains as an intergranular glassy phase. This intergranular film is approximately 1-1.5 nm thick and plays a key role in identifying the mechanical and high temperature properties of Si_3N_4 and related materials.²¹⁻²⁴ Moreover, the glassy grain boundary phase may exhibit different biochemical properties from the Si_3N_4 crystal itself, and there are also several studies supporting this.^{4,8,25}

An alternative for biomedical applications may be to select biocompatible sintering aids, such as Ca or Sr, in which only mechanical properties have been examined so far.²⁶ Additionally, it is believed that the cations from different sintering additives may affect its surface properties and therefore biochemical properties, in order to achieve their cation field strength (CFS) values. CFS values of rare earth (RE) cations with the same coordination number (CN) and valence are inversely proportional to ionic radii ($\text{CFS} = Z/r^2$ where Z = valence and r = ionic radius). Eventually, it is clear that it is important to carry out a systematic study on different sintering additives.

In this study, the effect of the glassy grain boundary phase on antibacterial behavior and biocompatibility properties was determined on Si_3N_4 materials to improve their use in the biomedical field. For this purpose, glasses with different sintering additives were prepared to mimic the grain boundary phase in Si_3N_4 systems. Although it is not entirely possible to mimic the glass composition at the grain boundary of silicon nitride (since nitrogen plays a fundamental role during sintering and the O:N ratio might change), this study aimed to shed light on the effect of additives, when the O:N ratio is constant. Biochemical and related properties of the glasses in the $X \pm \text{Ca} \pm \text{Si} \pm \text{Al} \pm \text{O} \pm \text{N}$ system (with $X = \text{Ca}, \text{Dy}, \text{Er}, \text{Eu}, \text{Nd}, \text{Sm}, \text{and Yb}$) with a standard cation composition were tested, and the results were compared.

2 | EXPERIMENTAL PROCEDURE

2.1 | Glass sample preparation

Glasses in the X-Ca-Si-Al-O-N system with a cation composition (in equivalent % - e/o) of 1X-27Ca-56Si-16Al (with $X = \text{Ca}, \text{Dy}, \text{Er}, \text{Eu}, \text{Nd}, \text{Sm}, \text{and Yb}$), containing five equivalent percent (e/o) of N were prepared. This means that the X cations were present in each glass at a 1 e/o, and the remaining modifying cation was Ca. The reason for using such a high amount of Ca was to reduce the glass transition temperature and prevent crystallization. Batches were homogenized in isopropanol by planetary ball mill using Si_3N_4 balls and afterwards dried in a rotary evaporator followed by sieving.

Samples having a diameter of 40 mm with 10-mm height were shaped by pressing under 30 MPa. Intensive care was paid to clean the surface impurities coming from the mold. The melting process of the samples was carried out in a flowing nitrogen atmosphere. All batches were calcined at 800°C for 1 h to remove volatiles or chemically absorbed water. The color change depending on the rare-earth metal cation used is given in Figure 1. All the samples in this study were used after cutting into small pieces to be tested, and only surface cleaning (ultrasonic cleaning in acetone, ethanol, and deionized water for 15 minutes each) was performed before the tests.

2.2 | Phase characterization, contact angle, and IEP measurements

Phase identification of the glass samples was performed by X-ray diffraction analysis (XRD) (RINT2200, Rigaku, Tokyo, Japan) with $\text{CuK}\alpha$ ($\lambda = 1.54056 \text{ \AA}$) radiation using a scan speed of $1^\circ/\text{min}$ between 20° and 70° .

In order to determine the surface and interfacial interaction that takes place between the glasses and liquid media, contact angle measurements were carried out. A drop shape analysis system (Phoenix 150 Contact angle measurement system) with analysis software was used. The system consisted of an optical tensiometer equipped with a CCD video camera having a specially designed optical system for reducing light scattering and mounting an easy camera with all direction adjustment. Drops were deposited on the surfaces, at room temperature, through a needle. The outline of the drops after 5 seconds was recorded and analyzed. Wetting measurements were carried out at the fifth second after the drop, to be able to make a good comparison between the samples.

Longer times were avoided because of either the importance of the early surface interaction between the fluid and the solid surface or to prevent changes of the contact angle deriving from secondary effects like solid/ liquid reactions or liquid evaporation.²⁷

Zeta potential measurements were carried out to determine the zeta potential as a function of pH and herein to determine the isoelectric point (IEP) for each material, using a ZetaSizer Nano ZS (Malvern Instruments Inc., UK). Powdered samples of 0.05 g were dispersed in 50-ml deionized (DI) water, individually. Prior to the measurement, the suspensions were ultrasonicated for 5 minutes. The initial pH, which was around 7, decreased and was adjusted through the addition of 1-M hydrochloric acid (HCl) and pH measurements of the ground glass and were averaged from three separate time measurements.

2.3 | Bacteria and cell culture studies

Three glass samples of each composition were tested against three types of bacteria: *S. aureus* (ATCC 25923), *E. coli* (ATCC 25922), and *Pseudomonas aeruginosa* (*P. aeruginosa*, ATCC 27853) by a broth dilution test to study the antibacterial properties of the glass samples. Among these bacteria, *E. coli* and *P. aeruginosa* are gram-negative, and *S. aureus* is gram-positive. All of the bacteria were obtained from the American Type Culture Collection (Manassas, VA). Separate media were inoculated with one colony of each bacteria and cultured on a shaking flask at 37°C for 24 h. Samples were put in a well plate and covered with the prepared bacteria solution at an initial concentration of 10^5 cells/ml, which was prepared using optical absorbance. Each system was tested using three samples. After incubation for 24 hours, samples were washed with








Ca	Dy	Er	Eu	Nd	Sm	Yb
						
Ca: Ca-Si-Al-O-N glass			28Ca: 56Si:16Al			
Dy: Dy-Ca-Si-Al-O-N glass			1Dy: 27Ca: 56Si:16Al			
Er: Er- Ca-Si-Al-O-N glass			1Er: 27Ca: 56Si:16Al			
Eu: Eu- Ca-Si-Al-O-N glass			1Eu: 27Ca: 56Si:16Al			
Nd: Nd- Ca-Si-Al-O-N glass			1Nd: 27Ca: 56Si:16Al			
Sm: Sm- Ca-Si-Al-O-N glass			1Sm: 27Ca: 56Si:16Al			
Yb: Yb- Ca-Si-Al-O-N glass			1Yb: 27Ca: 56Si:16Al			

FIGURE 1 Change in color as a function of X cation in glasses (chemical compositions are given in e/o)

a phosphate buffered solution (PBS) and introduced in proper tubes with a proper amount of PBS added and sonicated for 10 minutes followed by vortexing for 10 seconds before preparing four different dilutions (1:1000, 1:10 000, 1:100 000, and 1:1 000 000) of each sample. Three 10- μ l droplets of each dilution were dropped onto Petri dishes overlaid by solidified mixtures containing 1.5% of agar and 3.0% of TSB and were allowed to air dry for 15 minutes in a sterile environment. The plates were then incubated in a stationary incubator operating at 5% CO₂ and 37°C for 12 hours until the colonies formed and reached a size that could be counted. Because the sizes of the samples were not totally equal to each other, area calculations were carried out and normalized by the bacteria results. When calculating the area of the samples, a surface that was in contact with the base of the well plate was subtracted because the bacteria were not able to attach to that surface.

Cell viability tests were also determined on the same glasses using human fetal osteoblasts (hFOB 1.19, CRL-11372; American Type Culture Collection) at a passage number of 8. For the viability assays, osteoblasts were lifted from the tissue-culture, suspended in cell culture media, and counted using a hemocytometer. Samples were distributed within a 48-well plate, and 0.5 ml of a 50 000 hFOB cells/ml media suspension were injected into the wells containing the glass samples. A 4-h incubation period was selected to evaluate the level of hFOB adhesion, and three post-incubation times (1, 3, and 5 days) were applied to measure the proliferation. After 1, 3, and 5 days of culture, samples were transferred to new well plates and immersed in a 16.7% v/v MTS [3-(4,5-dimethylthiazol-2-yl)-5-(3-carboxymethoxyphenyl)-2-(4-sulfophenyl)-2H tetrazolium, inner salt; Promega] solution (1-ml MTS: 5-ml DMEM-F12). Test specimens in MTS were incubated in a humidified atmosphere at 5% CO₂ and 37°C. After reduction of the tetrazolium compound, the bulk solutions surrounding each test specimen were re-suspended through continuous pipetting to ensure homogeneity in the color saturation, and 200 μ l from each solution

were deposited into the wells of clear bottom 96-well plates. Absorbance readings at λ equal to 490 nm were immediately obtained using a spectrophotometer. All procedures involving MTS were performed in the dark to avoid discoloration of the reagent due to light-sensitivity. All experiments were run in triplicate and repeated at least three times. Results of percent viability as a function of varying times ranging between 1 and 5 days were compared.

2.4 | Statistical analysis

All the reported values represent the average of three independent experiments. Standard errors of the mean were calculated in order to define data uncertainty, and representative error bars were included for all data figures. Analysis of the results was carried out using the Student's *t*-test, with a significance level of $p < 0.05$.

3 | RESULTS

3.1 | Phase characterization, contact angle, and IEP measurements

XRD results of the glasses, in the form of a crushed powder, were analyzed to detect the presence of any crystalline phases. Crystalline phase formation was not observed in any of the glasses produced, rather a 100% amorphous phase was achieved. A typical XRD pattern for all the produced glasses is shown in Figure 2.

Figures 3 and 4 show the contact angle measurement results and two wetting images of the glasses produced, respectively. In Figure 3, the cations are arranged on the *x*-axis according to the increasing CFS value. The contact angle values obtained on the glass showed that the wetting contact angle decreased as the CFS value increased.

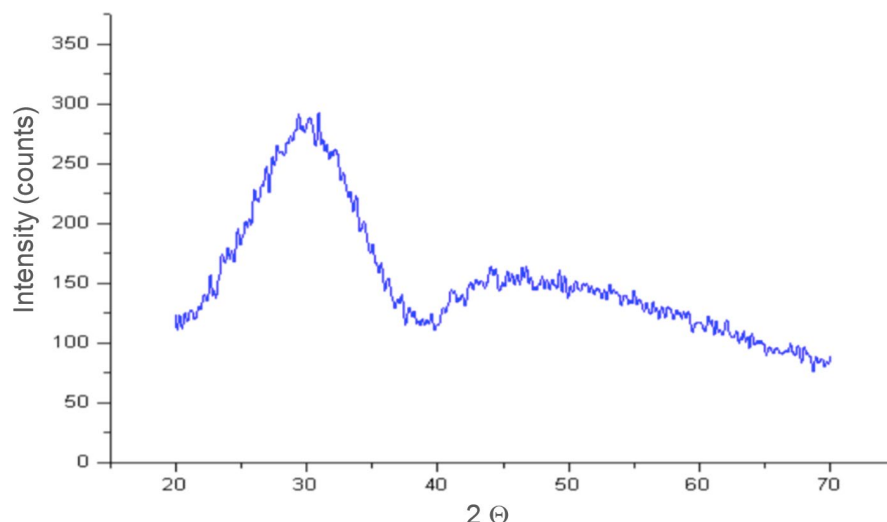


FIGURE 2 A typical X-ray diffraction (XRD) pattern for all the produced glasses

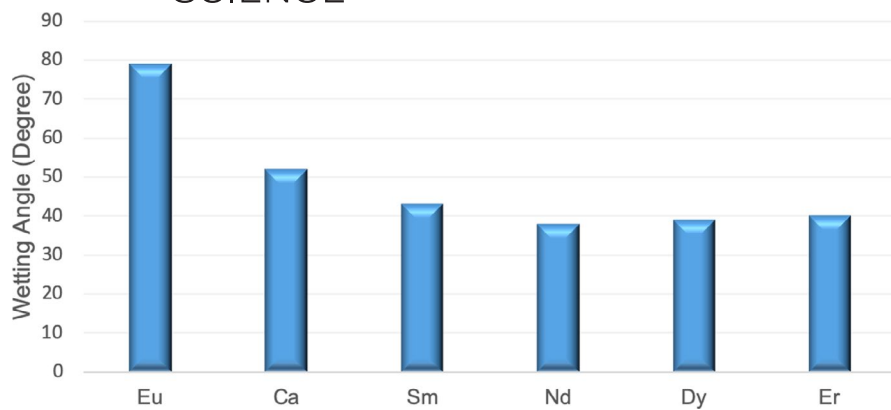


FIGURE 3 Contact angle measurement results of the glass samples with various additives



FIGURE 4 Wetting contact angle images for the Eu and Nd containing glasses

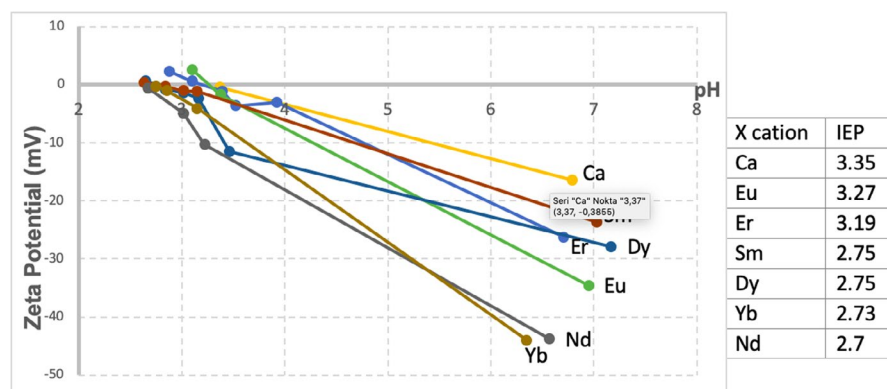


FIGURE 5 The influence of pH on the zeta potential of glasses with various cations. IEP, isoelectric points

Figure 5 shows the zeta-potential as a function of pH for glasses having different cations. All of the produced glasses revealed negative zeta-potentials at physiological pH values of ~7.4. IEPs were found by the intersection of the trend lines on the pH axis as 3.35, 3.27, 3.19, 2.75, 2.75, 2.73, and 2.7 for Ca, Eu, Er, Sm, Dy, Yb, and Nd, respectively.

3.2 | Bacteria and cell culture results

Bacteria test results are given in Figure 6. The y-axis of the graphs represents the counted bacteria colony forming units

per square millimeter, CFU/mm², and the dopants given on the x-axis are according to increasing CFS values. Our results were compared with the control data obtained by Robinson et al²⁸ with the same bacteria strains and the same bacterial initial concentration. Results revealed that there was no correlation between bacteriostatic behavior and CFS. There was also no sharp contrast in gram-positive and gram-negative bacteria responses. Impressively, it was observed that tests on the Eu-doped glass were unfavorable for all types of bacteria (promoting their colonization) and Nd resulted in preferable bacteria responses (reducing their colonization). The second best choice for reducing bacteria colonization was Ca doping.

FIGURE 6 Antibacterial test results of glass samples, having different kinds of dopants (classified based on gram-positive and gram-negative bacteria) (Data = \pm SD; $n = 3$)

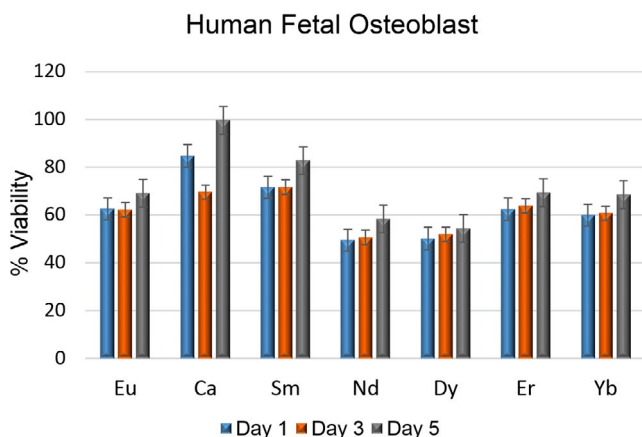
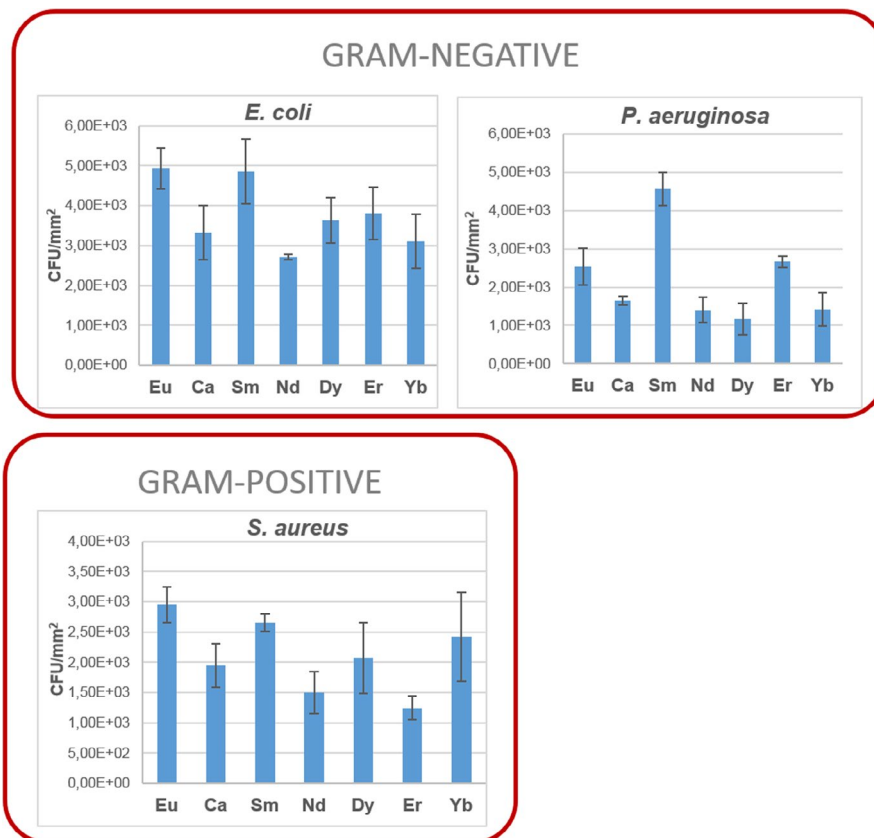


FIGURE 7 Cell culture test results of the glass samples (Data = \pm SD; $n = 3$, same samples different times)

Cell culture tests used the same glasses with human fetal osteoblasts. Results of percent viability as a function of varying times ranged between 1 to 5 days and are given in Figure 7.

4 | DISCUSSION

Initial contact angle measurements of the glasses showed that the wetting angles decreased as the CFS value increased,

thereby achieving more hydrophilic surfaces. Incorporating especially high CFS modifiers to the glass structure, such as trivalent yttrium and lanthanides, can be desirable for structural applications because the resulting glass often has elevated corrosion resistance, hardness, glass transition temperatures, and coefficients of thermal expansion.²⁹ The contact angle results of this study showed that the glasses obtained with trivalent cations gave better results in terms of wetting than the glasses containing divalent cations.

The nature of the intermolecular forces between the solid surface and the liquids depend on the topography of the acting surface and the surface chemistry. However, since in this study, glass samples are at issue, roughness data would not have a significant influence on wetting behavior. Therefore, the wetting results should be attributed to the change in surface chemistry as a fact of the different additives used. The trend of contact angle decreases as CFS increases is related to the increasing bonding energy and bond strengths as the valance increases. The effect of some of the rare-earth cations on the properties of oxynitride glasses and change in glass transition temperature as a function of CFS was previously investigated.³⁰⁻³¹ According to those results, there was a linear increase in glass transition temperature as the CFS increased which is evidence of the change in bond strength.

The IEP is known as the pH at which a material displays zero net surface charge. When the IEP of the material is higher than the pH value of its environment, the surface

exhibits a net negative charge and vice versa. Negative surface charges of biomedical Si_3N_4 plays an important role depending on two issues: (i) antibacterial behavior; most of the bacteria exhibit a negative charge at physiological pH (which is ~ 7.4), so it will be repulsed if the surface of the biomaterial is also negatively charged³² and (ii) bioactivity; according to the mechanism for osteointegration proposed by Kim et al.,³³ apatite formation can be observed on materials exhibiting a negative surface charge at a physiological pH. Therefore, surface charges of the fine particulate glass samples were measured as a function of pH to explain bacterial responses.

The IEPs achieved in this study (Figure 5) are much lower than the pure Si_3N_4 that is around ~ 9.7 ³⁴ as a result of the high concentration of amine functional groups (Si-NH_2) on the surface and pretty close to pure SiO_2 which is around 3.1 due to the high concentration of silanol functional groups (Si-OH).³⁵ The effect of functional groups at the surface of Si_3N_4 was previously reported when the material was subjected to thermal, chemical, and mechanical treatments.³⁶ For any kind of treatment resulting in decreasing O/Si and increasing N/Si atomic ratios, the IEPs of these variously treated samples increased (as the surfaces transitioned from resembling pure SiO_2 to pure Si_3N_4). In our study, the results indicated that the silanol groups predominated the amines on the oxynitride glass surfaces.

Taking into account the effect of the cation type, it is obvious that the divalent modifiers (Ca and Eu) had slightly higher IEPs. When a divalent modifier was used, every M^{2+} ion must have two neighboring nonbridging oxygens (NBOs), which is much more tightly bonded to the network. However, trivalent modifying RE cations have a strong affinity for oxygen, and NBOs are formed (RE-O-Si bonds) at low concentrations.³⁷ Therefore, relatively lower IEPs were obtained in glasses containing trivalent cations.

According to the bacteria test results, no correlation was observed between bacteriostatic behavior and CFS. Bacterial

adhesion to a glass surface depends on various properties, such as surface energy, wetting behavior, and surface charge. Increasing ionic strength generally increases bacterial adhesion by reducing the repulsive forces between the negatively charged bacteria and substrate surfaces.³⁸⁻⁴³ The magnitude of the repulsion is expected to increase as the magnitude of the surface charge increases. It has also been revealed that the density of the adhering cells increases when the pH of the suspending medium is brought near the IEP of the substrate surface. For this study, when the wetting behavior and the IEPs of the glasses are taken into consideration to understand bacteria adhesion, the results are in a good correlation. Nd glass, which acted the most favorably by means of reducing microbial adhesion and colonization for all kinds of bacteria, was also the one that had the lowest IEP and was the most hydrophilic one. Similarly, the divalent cation Eu was less favorable for bacteria colonization and had one of the highest IEPs (after another divalent cation, Ca) and had a dramatically high wetting angle.

According to the cell culture tests, Nd, the best acting cation for the antibacterial response, was the one with the least osteoblast viability. Interestingly, only Ca seemed to be the best option as a doping element considering both bacteria and osteoblast viability results at the same time. The key results of this study are schematically summarized in Figure 8, where the bacteria test results are normalized for the same type of bacteria and superimposed with the osteoblast viability results in the same graph. Results clearly showed that the best choice of additive in terms collectively minimizing bacteria colonization and maximizing osteoblast viability was Ca.

5 | CONCLUSION

In this study, the antibacterial behavior and osteoblast viability of a series of oxynitride glasses were investigated as

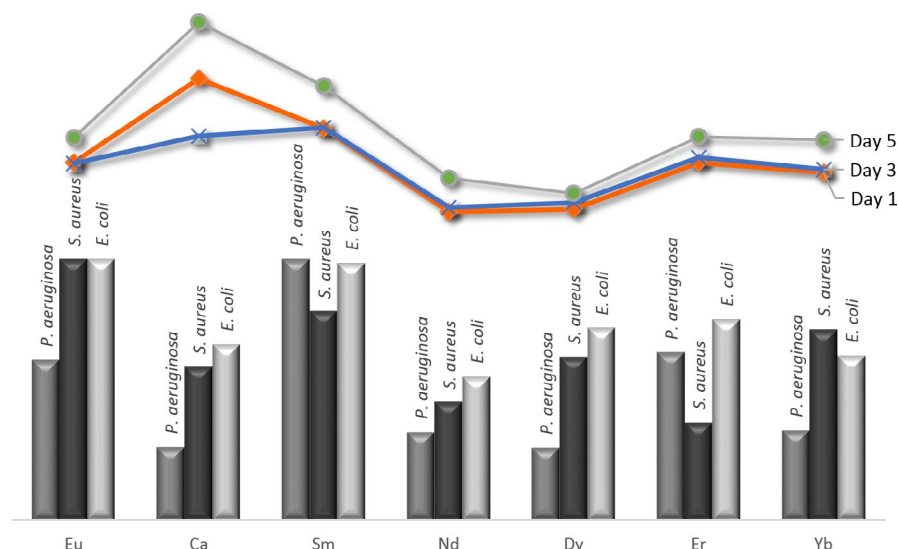


FIGURE 8 Combination of normalized bacteria results (lower bars) with human fetal osteoblasts (upper lines)

a function of different cation addition into the glass network. Besides bacterial and cell culture tests, the wetting behavior and IEP values affecting biochemical properties were also examined. As a result of the bonding energy and bond strength, the wetting angle dramatically decreased with an increase in CFS value. All of the glasses revealed negative zeta-potentials at physiological pH values. Depending on the results, silanol groups are thought to predominate the amines on all glass surfaces. EIPs of the glasses showed that the divalent modifiers (Ca and Eu) had a slightly higher IEPs compared to trivalent ones. Bacteriostatic behavior within gram-positive *S. aureus* and gram-negative *E. coli* as well as *P. aeruginosa* showed that divalent Eu-doped glass, which had a relatively high IEP and the highest wetting angle among all glasses, was unfavorable for all types of bacteria. Trivalent Nd-doped glass, which had the lowest IEP and wetting angle, resulted in a preferable response, regardless of the bacteria type, so it can be useful in preventing biofilm formation and bacterial proliferation when used as a sintering additive to Si_3N_4 and SiAlON ceramics. The human fetal osteoblast viability results indicated that Ca-oxynitride glasses provided good osteoblast viability after 1, 3, and 5 days as well as an effective bactericidal activity against both gram-positive and gram-negative bacteria making Ca a very useful dopant for Si_3N_4 and SiAlON bioceramics.

ACKNOWLEDGMENTS

One of the authors, Seniz R. Kushan Akin, would like to thank The Scientific and Technological Research Council of Turkey (TUBITAK) for funding her studies through the 2219 Fellowship Programme.

ORCID

Seniz R. Kushan Akin  <https://orcid.org/0000-0002-0287-1139>

[org/0000-0002-0287-1139](https://orcid.org/0000-0002-0287-1139)

Emrah Dolekcekic  <https://orcid.org/0000-0001-5833-1169>

[org/0000-0001-5833-1169](https://orcid.org/0000-0001-5833-1169)

Thomas J. Webster  <https://orcid.org/0000-0002-2028-5969>

[org/0000-0002-2028-5969](https://orcid.org/0000-0002-2028-5969)

REFERENCES

- Kue R, Sohrabi A, Nagle D, Frondoza C, Hungerford D. Enhanced proliferation and osteocalcin production by human osteoblast-like MG63 cells on silicon nitride ceramic discs. *Biomaterials*. 1999;20:1195–201.
- Pezzotti G, Oba N, Zhu W, Marin E, Rondinella A, Boschetto F, et al. Human osteoblasts grow transitional Si/N apatite in quickly osteointegrated Si_3N_4 cervical insert. *Acta Biomater*. 2017;64:411–20.
- Marin E, Horiguchi S, Zanocco M, Boschetto F, Rondinella A, Zhu W, et al. Bioglass functionalization of laser-patterned bioceramic surfaces and their enhanced bioactivity. *Heliyon*. 2018;4:e01016.
- Guedes Silva CC, Rodas ACD, Silva AC, Ribeiro C, Souza Carvalho FM, Higa OZ, et al. Microstructure, mechanical properties and in vitro biological behavior of silicon nitride ceramics. *Mater Res*. 2018;21(6):e20180266.
- Lal S, Caseley EA, Hall RM, Tipper JL. Biological impact of silicon nitride for orthopaedic applications: Role of particle size, surface composition and donor variation. *Sci Rep*. 2018;8:9109.
- Guedes Silva CC, Higa OZ, Bressiani JC. Cytotoxic evaluation of silicon nitride-based ceramics. *Mater Sci Eng, C*. 2004;24(5):643–6.
- Santos C, Ribeiro S, Daguano JKMF, Rogero SO, Strecker K, Silva CRM. Development and cytotoxicity evaluation of SiAlONs ceramics. *Mater Sci Eng, C*. 2007;27(1):148–53.
- Mazzocchi M, Bellosi A. On the possibility of silicon nitride as a ceramic for structural orthopaedic implants. Part I: processing, microstructure, mechanical properties, cytotoxicity. *J Mater Sci: Mater Med*. 2008;19:2881–7.
- Precnerová M, Bodišová K, Frajkorová F, Galusková D, Nováková ZV, Vojtaššák J, et al. In vitro bioactivity of silicon nitride-hydroxyapatite composites. *Ceram Int*. 2015;41(6):8100–8.
- Gorth DJ, Puckett S, Ercan B, Webster TJ, Rahaman M, Bal BS. Decreased bacteria activity on Si_3N_4 surfaces compared with PEEK or titanium. *Int J Nanomed*. 2012;7:4829–40.
- Bock RM, Jones EN, Ray DA, Bal BS, Pezzotti G, McEntire BJ. Bacteriostatic behavior of surface-modulated silicon nitride in comparison to polyetheretherketone and titanium. *J Biomed Mater Res Part A*. 2017;105.
- Webster TJ, Patel AA, Rahaman MN, Bal BS. Anti-Infective and osteointegration properties of silicon nitride, poly (ether ether ketone), and titanium implants. *Acta Biomater*. 2012;8:4447–54.
- Griss P, Wener E, Heimke G. Alumina ceramic, bioglass, and silicon nitride: A comparative biocompatibility study. In: Hastings GW, Williams DF, editors. *Mechanical properties of biomaterials*. New York: John Wiley & Sons; 1980. p. 217–26.
- Howlett CR, McCartney E, Ching W. The effect of silicon nitride ceramic on rabbit skeletal cells and tissue. An in vitro and in vivo investigation. *Clin Orthop Relat Res*. 1989;244:293–304.
- Mobbs RJ, Rao PJ, Phan K, Hardcastle P, Choy WJ, McCartney ER, et al. Anterior lumbar interbody fusion using reaction bonded silicon nitride implants: Long-term case series of the first synthetic anterior lumbar interbody fusion spacer implanted in humans. *World Neurosurg*. 2018;120:256–64.
- Rahaman M, Xiao W. Silicon nitride bioceramics in healthcare. *Int J Appl Ceram Technol*. 2018;15:861–72.
- Boschetto F, Adachi T, Horiguchi S, Fainozzi D, Parmigiani F, Marin E, et al. Monitoring metabolic reactions in *Staphylococcus epidermidis* exposed to silicon nitride using in situ time-lapse Raman spectroscopy. *J Biomed Opt*. 2018;23(5):056002.
- Rondinella A, Marin E, McEntire BJ, Bock R, Bal BS, Zhu W, et al. Bioceramics are not bioinert: the role of oxide and non-oxide bioceramics on the oxidation of UHMWPE components in artificial joints. *Key Eng Mater*. 2018;782:165–75.
- Marin E, Adachi T, Boschetto F, Zanocco M, Rondinella A, Zhu W, et al. Biological response of human osteosarcoma cells to Si_3N_4 -doped bioglasses. *Mater Des*. 2018;159:79–89.
- Liu T, Zhou X, Qi F, Li L, Li Q, Shi G, et al. The effect of T-ZnOw addition on the microstructure, mechanical and antibacterial properties of Si_3N_4 ceramics for biomedical applications. *Ceram Int*. 2019;45:2393–9.
- Becher PF, Sun EY, Plucknett KP, Alexander KB, Hsueh CH, Lin HT, et al. Microstructural design of silicon nitride with improved

- toughness: I, effects of grain shape and size. *J Am Ceram Soc.* 1998;81(11):2821–30.
22. Becher PF, Painter GS, Sun EY, Hsue CH, Lance MJ. The importance of amorphous intergranular films in self-reinforced Si_3N_4 ceramics. *Acta Mater.* 2000;48(18–19):4493–9.
23. Yang J, Yang JF, Shan SY, Gao JQ, Ohji T. Effect of sintering additives on microstructure and mechanical properties of porous silicon nitride ceramics. *J Am Ceram Soc.* 2006;89(12):3843–5.
24. Han W, Li Y, Chen G, Yang Q. Effect of sintering additive composition on microstructure and mechanical properties of silicon nitride. *Mater Sci Eng, A.* 2017;700:19–24.
25. Amaral M, Lopes MA, Santos JD, Silva RF. Wettability and surface charge of Si_3N_4 -bioglass composites in contact with simulated physiological liquids. *Biomaterials.* 2002;23(20):4123–9.
26. Pettersson M, Pakdaman Z, Engqvist H, Liu Y, Shen Z, Östhols E. Spark plasma sintered β -phase silicon nitride with Sr and Ca as a sintering aid for load bearing medical applications. *J Eur Ceram Soc.* 2012;32(11):2705–9.
27. Mazzocchi M, Gardini D, Traverso PL, Faga MG, Bellosi A. On the possibility of silicon nitride as a ceramic for structural orthopaedic implants. Part II: chemical stability and wear resistance in body environment. *J Mater Sci Mater Med.* 2008;19:2889–901.
28. Robinson DA, Griffith RW, Shechtman D, Evans RB, Conzemius MG. In vitro antibacterial properties of magnesium metal against *Escherichia coli*, *Pseudomonas aeruginosa* and *Staphylococcus aureus*. *Acta Biomater.* 2010;6:1869–77.
29. Lofaj F, Satet R, Hoffmann MJ, Lopez ARA. Thermal expansion and glass transition temperature of the rare-earth doped oxynitride glasses. *J Eur Ceram Soc.* 2004;24(12):3377–85.
30. Menke Y, Peltier-Baron V, Hampshire S. Effect of rare-earth cations on properties of sialon glasses. *J Non-Cryst Solids.* 2000;276:145–50.
31. Orhun C, Dolekcekic E. Investigation on the Effect of Rare Earth (RE) cation to the (Re+Ca) Sialon glasses. *Anadolu University J. Sci. and Tech.–A. App. Sci and Eng.* 2012;13(2):47–54.
32. Arafat A, Schroën K, de Smet LC, Sudhölter EJ, Zuilhof H. Tailor-made functionalization of silicon nitride surfaces. *J Am Chem Soc.* 2004;126:8600–1.
33. Kim HM, Himeno T, Kawashita M, Lee JH, Kokubo T, Nakamura T. Surface potential change in bioactive titanium metal during the process of apatite formation in simulated body fluid. *J Biomed Mater Res A.* 2003;67(4):1305–9.
34. Hackley VA, Wang PS, Malghan SG. Effects of soxhlet extraction nitride powders on the surface oxide layer of silicon nitride powders. *Mater Chem Phys.* 1993;36:112–8.
35. Givens BE, Xu Z, Fiegel J, Grassian VH. Bovine serum albumin adsorption on SiO_2 and TiO_2 nanoparticle surfaces at circumneutral and acidic pH: A tale of two nano-bio surface interactions. *J Colloid Interface Sci.* 2017;493:334–41.
36. Hamadi F, Latrache H, Mabrouki M, Elghmari A, Outzourhit A, Ellouali M, et al. Effect of pH on distribution and adhesion of *Staphylococcus aureus* to glass. *J Adhes Sci Technol.* 2005;19(1):73–85.
37. Becher PF, Hampshire S, Pomeroy MJ, Hoffmann MJ, Lance MJ, Satet RL. An overview of the structure and properties of silicon-based oxynitride glasses. *Int J App Glass Sci.* 2011;2(1):63–83.
38. Jucker BA, Harms H, Zehnder AJB. Adhesion of the positively charged bacterium *Stenotrophomonas (Xanthomonas) maltophilia* 70401 to glass and Teflon. *J Bacteriol.* 1996;178:5472–9.
39. Fletcher M. The application of interference reflection microscopy to the study of bacterial adhesion to solid surfaces. *Biodeterioration.* 1988;7:31–5.
40. Fletcher M. Attachment of *Pseudomonas fluorescens* to glass and influence of electrolytes on bacterium-substratum separation distance. *J. Bacteriol.* 1998;170:2027–30.
41. Rijnaarts HHM, Norde W, Bouwer EJ, Lyklema J, Zehnder AJB. Bacterial adhesion under static and dynamic conditions. *Appl Environ Microbiol.* 1993;59:3255–65.
42. Rijnaarts HHM, Norde W, Bouwer EJ, Lyklema J, Zehnder AJB. Reversibility and mechanism of bacterial adhesion. *Colloids Surf, B.* 1995;4(1):5–22.
43. Rijnaarts HHM, Norde W, Bouwer EJ, Lyklema J, Zehnder AJB. Bacterial deposition in porous media: effects of cell-coating, substratum hydrophobicity and electrolyte concentration. *Environ Sci Technol.* 1996;30(10):2877–83.

How to cite this article: Kushan Akin SR, Dolekcekic E, Webster TJ. Antibacterial behavior of oxynitride glasses as a glassy grain boundary phase for silicon nitride-based ceramics. *Int J Appl Glass Sci.* 2021;12:328–336. <https://doi.org/10.1111/ijag.15902>